



A novel radiographic classification of severe spinal curvatures exceeding 100°: the Omega (Ω), gamma (γ) and alpha (α) deformities

Isaac Obiri Karikari¹ · Henry Pang² · Kwadwo Poku Yankey³ · Henry Ofori Duah³ · Harry Akoto³ · Rick Hodes⁴ · Oheneba Boachie-Adjei³ · FOCOS Spine Research Group³

Received: 25 September 2018 / Revised: 16 January 2019 / Accepted: 24 March 2019
© The Author(s) 2019

Abstract

Purpose For spine curvatures with Cobb angles $> 100^\circ$, curve classification and characterization become more difficult with conventional radiographs. 3-D computerized axial tomography scans add relevant information to categorize and describe a new classification to aid preoperative assessment in communication and patient evaluation. The purpose of this study is to describe a radiographic classification system of curves exceeding 100° .

Methods A consecutive series of patients with curves exceeding 100° underwent a full spine radiographic review using conventional radiographs and 3-D CT. A descriptive analysis was performed to categorize curves into 4 main types (1, 2, 3 and 4) and 6 subtypes (1C, 1S, 1CS, 2P, 2D and 2PD) based on the location of the Cobb angle of the major scoliotic and kyphotic deformity as well as the location of the upper/lower end vertebra relative to the apical vertebra.

Results A total of 98 patients met the inclusion criteria. There were 51 males and 47 females with an average age of 17.8 ± 4.5 years. The diagnosis included idiopathic (48); congenital (24); neuromuscular (4); and neurofibromatosis (2). The mean major coronal and sagittal Cobb (kyphosis) were $131.2^\circ \pm 23.4^\circ$ and 154 ± 45.6 , respectively. The classification scheme yielded 4 main types (1, 2, 3 and 4) and 6 subtypes under types 1 and 2 (1C, 1S, 1CS, 2P, 2D and 2PD).

Conclusions Our study describes a novel method of classifying severe spinal curvatures exceeding 100° using erect AP/lateral radiographs and 3-D CT reconstructive images. We hope that the descriptive analysis and classification will expand our understanding of these complex deformities.

Graphical abstract

These slides can be retrieved under Electronic Supplementary Material.

Spine Journal

Key points

1. Kyphoscoliosis
2. Classification
3. Spinal deformity

Spine Journal

Type	Coronal	Sagittal	LEV at or below apex	LEV at above apex
1C	$>100^\circ$	$<100^\circ$	No	No
1S	$<100^\circ$	$>100^\circ$	No	No
1CS	$>100^\circ$	$>100^\circ$	No	No
2P (partial Omega)	$>100^\circ$	$>100^\circ$	Yes	No
2D (half omega)	$>100^\circ$	$>100^\circ$	No	Yes
2PD (full omega)	$>100^\circ$	$>100^\circ$	Yes	Yes
3 (Gamma)	$<100^\circ$	$>180^\circ$	Yes	Yes
4 (Alpha)	$<100^\circ$	$>180^\circ$	Yes	Yes

Spine Journal

Take Home Messages

1. Current and existing classification schemes cannot be easily applied to severe kyphoscoliosis.
2. Severe kyphoscoliosis can be classified using a combination of radiographs and 3-D CT.
3. Classification schemes facilitate communication, research and aid in the development of treatment protocols for complex pathologies.

Karikari IO, Pang H, Yankey KP, Duah HO, Akoto H, Hodes R, Boachie-Adjei O, FOCOS Spine Research Group (2019) A Novel Radiographic Classification of Severe Spinal Curvatures Exceeding 100 degrees: The Omega (Ω), Gamma (γ) and Alpha (α) deformities. Eur Spine J.

Keywords Kyphoscoliosis · Omega deformities · Scoliosis · Kyphosis · Halo-gravity traction

Electronic supplementary material The online version of this article (<https://doi.org/10.1007/s00586-019-05963-w>) contains supplementary material, which is available to authorized users.

Extended author information available on the last page of the article

Introduction

Classification schemes for the musculoskeletal system are vital in assessing the natural history, treatment and prognosis of various conditions [1, 2]. Moreover, classification

schemes allow for efficient communication between treating clinicians and allow for consistency in research studies. The most popular and widely used classification systems in the treatment of scoliosis are the King–Moe and Lenke classifications [3, 4]. King et al. introduced the first set of classifications in 1983 for idiopathic scoliosis, the King–Moe classification, which categorized the thoracic curvature into types I–V. Later in 2001, Lenke et al. developed a three-component classification, for adolescent idiopathic scoliosis (AIS) that incorporates curve type, a lumbar spine modifier and a sagittal thoracic modifier [4]. The addition of sagittal modifiers enhances the utility of Lenke’s classification by addressing limitations of the King–Moe’s classification for selection fusion in AIS patients.

While the King and Lenke classifications are instrumental in treatment of AIS, a limitation of both classifications is their applicability to severe kyphoscoliosis. This subset of patients with spinal curvatures exceeding 100° in coronal and/or sagittal planes exhibits radiographic and clinical characteristics that are unique to this deformity and present significant treatment challenges. In adult spinal deformity, Schwab and associates of the ISSG have attempted to classify adult spine deformity utilizing the coronal, sagittal and pelvic parameters to aid in treatment methods, selection and prognostication [5]. More recently, Lamartina et al. and Berjano et al. have also provided an adult deformity classification with an emphasis on sagittal alignment and degenerative segment disease, respectively [6, 7]. However,

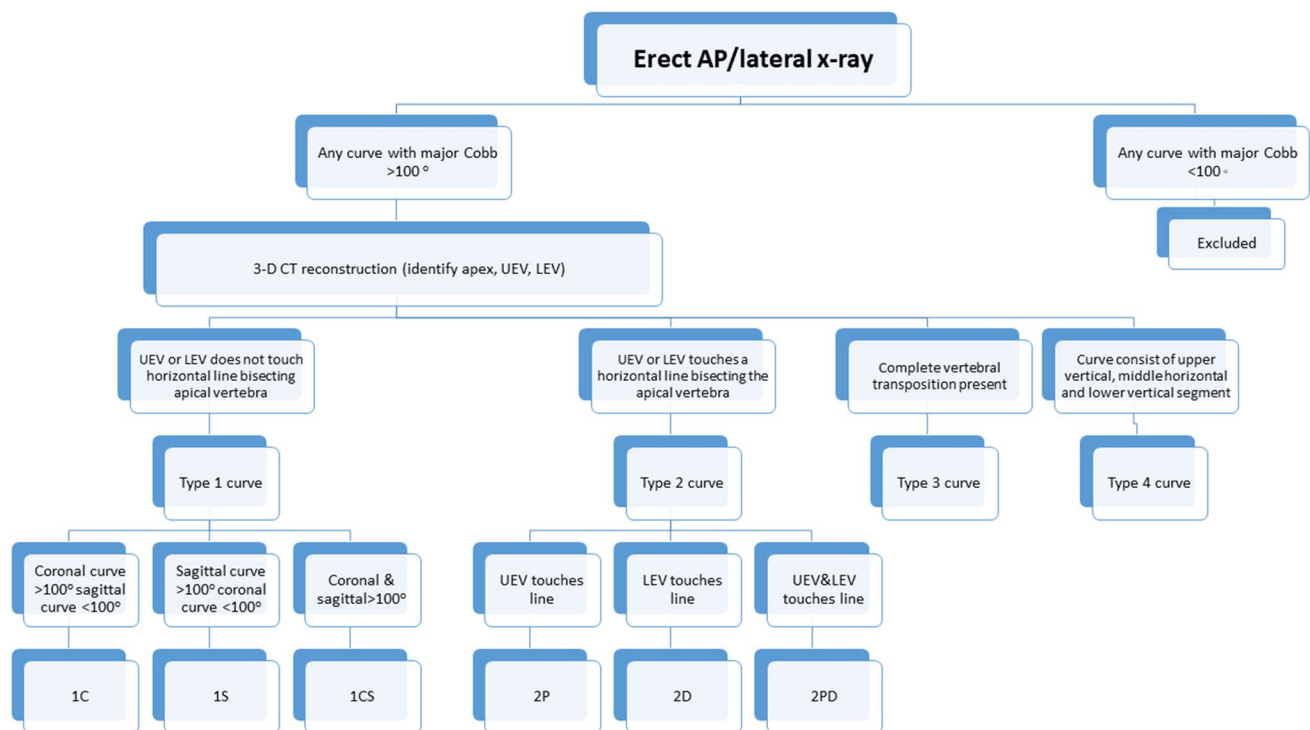


Fig. 1 Classification algorithm used to classify curve types in this study

Table 1 Summary of classification types

Type	Coronal	Sagittal	UEV touches bisecting horizontal apical line	LEV touches bisecting horizontal apical line
1C	> 100°	< 100°	No	No
1S	< 100°	> 100°	No	No
1CS	> 100°	> 100°	No	No
2P (partial omega)	> 100°	> 100°	Yes	No
2D (half omega)	> 100°	> 100°	No	Yes
2PD (full omega)	> 100°	> 100°	Yes	Yes
3 (gamma)	< 100°	> 180°	Yes	Yes
4 (alpha)	< 100°	> 180°	Yes	Yes

Table 2 Patient demographics and preoperative variables

Variables	Total (n=98)	1C (n=9)	1S (n=2)	1CS (n=43)	2P (n=21)	2D (n=2)	2PD (n=1)	Gamma (n=16)	Alpha (n=4)
Age (years)	17.8±4.5	17.7±3.7	13.2	17.5 ± 4	18.9 ± 5.8	19.5	22.5	17.9±4.1	17.2±4.2
Sex (no.)	F (51) M (47)	F (8) M (1)	F (1) M (1)	F (20) M (23)	F (8) M (13)	F (2) M (0)	F (1) M (0)	F (9) M (7)	F (2) M (2)
BMI (kg/m ²)	18.4±2.9	19.4±3.3	15.7	18.2 ± 3.2	17.5 ± 2.4	19.8	17	19.4±2.7	21.5±1.2
Median pre-op Risser [IQR]	5 [4–5]	4 [3–4]	0	5 [3–5]	5 [4.75–5]	5	5	5 [4.75–5]	N/A
Pre-op length in halo (days)	111.3 ± 41.5	104.3±59.9	42	92.8 ± 28.4	126.1 ± 25.5	117.5	239	125±49.6	134.0±47.0
Diagnosis: congenital (no.)	36	2	2	13	6	1	0	11	0
Diagnosis: idiopathic (no.)	51	6	0	29	11	1	1	1	2
Diagnosis: neuromuscular (no.)	4	1	0	1	2	0	0	0	0
Diagnosis: neurofibromatosis (no.)	7	0	0	0	2	0	0	3	1
Diagnosis: post-TB (no.)	2	0	0	0	0	0	0	1	1

there are severe and complex deformities that span various diagnostic categories in both adolescent and adult for whom conventional classifications do not lend themselves to simple descriptive terminology and treatment methods.

Herein, we describe a new classification scheme of severe kyphoscoliosis by utilizing both conventional radiographs

and 3-dimensional (D) CT scans to better define the curve characteristics in both coronal and sagittal planes for curves exceeding 100°. We hope that the findings in this study will provide some insight into the unique characteristics and treatment strategies in this very challenging patient population.

Table 3 Preoperative radiographic data

Variables	Total (n=98)	1C (n=9)	1S (n=2)	1CS (n=43)	2P (n=21)	2D (n=2)	2PD (n=1)	Gamma (n=16)	Alpha (n=4)
Major Cobb°	131.2 ± 23.4	120±8.2	79.6	127.7 ± 15.8	145.9 ± 27.6	135.6	171	N/A	N/A
Curve region (no.)	T (54) TL (44)	T (3) TL (6)	T (1) TL (1)	T (28) TL (15)	T (14) TL (7)	T (1) TL (1)	T (1)	T (5) TL (11)	T (1) TL (3)
Direction of curve L/R (no.)	L (27) R (71)	L (2) R (7)	L (1) R (1)	L (20) R (23)	L (4) R (17)	L (0) R (2)	L (0) R (1)	N/A	N/A
Median levels [IQR]	8 [7–8]	7 [6–8]	7	7 [7–8]	8 [7–9]	9	8	N/A	N/A
Minor Cobb°	69.4±18.2	76.4±12.3	44.5	68.6 ± 13.5	71.3 ± 27.1	65.6	69	N/A	N/A
Direction of curve L/R (No.)	L (53) R (25)	L (7) R (2)	L (1) R (1)	L (25) R (18)	L (17) R (4)	L (2) R (0)	L (1) R (0)	N/A	N/A
Median levels [IQR]	6 [5–6]	5 [5–6.25]	5	6 [5–6]	6 [5–6]	5	5	N/A	N/A
Kyphosis°	154±45.6	81.6±18.1	113.2	131.8 ± 21.0	169.3 ± 14.5	157.5	176	216.7±22.2	238.0±6.5
Median levels [IQR]	7 [6–8]	7 [7–8]	6	8 [7–9]	8 [7–9]	8	8	4 [3.75–6]	5 [4.75–5.75]

Methods

Study design

This is a prospective case series of seventy-eight consecutive patients with coronal and/or sagittal curves exceeding 100° who were treated from January 2012 to December 2015. All patients were evaluated at a single specialty hospital in West Africa. Institutional Review Board (IRB) approval was obtained prior to initiation of the study. The inclusion criteria were: (1) curve magnitude $> 100^\circ$ in sagittal and/or

coronal planes on preoperative erect AP/lateral X-rays, (2) visible radiographic images permissive to accurate radiographic measurements, (3) the presence of 3-D CT reconstructive images.

Demographic information including age, sex, body mass index (BMI) and preoperative diagnosis was collected. Radiographic data from erect anterior–posterior (AP) and lateral views and 3-D CT reconstructions were collected and analyzed. Pre- and post-halo-gravity traction X-rays were also analyzed to provide a surrogate for curve flexibility.

Table 4 Post-traction results

Variables	Total (n = 100)	1C (n = 9)	1S (n = 2)	1CS (n = 43)	2P (n = 21)	2D (n = 2)	2PD (n = 1)	Gamma (n = 16)	Alpha (n = 4)
Length in traction (days)	106.2 \pm 38.2	104.3 \pm 59.9	42	92.8 \pm 28.4	126.1 \pm 25.5	117.5	239	125 \pm 49.6	134.0 \pm 47.0
Major Cobb $^\circ$	92.9 \pm 16.5	89.5 \pm 5.5	62.4	92.6 \pm 15.3	92 \pm 14	109.2	134	N/A	N/A
Correction (%)	30.0 \pm 11.4	26 \pm 2.2	30.5	28.1 \pm 10.9	35.6 \pm 12.3	20.1	22	N/A	N/A
Minor Cobb $^\circ$	50.3 \pm 16.6	67.7 \pm 22.1	25.5	50 \pm 10.7	46.5 \pm 20.7	57.9	34	N/A	N/A
Correction (%)	27.6 \pm 21.0	19.7 \pm 16.4	42.8	27.5 \pm 20.2	32.8 \pm 18.9	11.1	51	N/A	N/A
Kyphosis $^\circ$	117.4 \pm 48.5	60.3 \pm 26.2	67.8	91.5 \pm 17.6	113.8 \pm 13.6	141.1	171	157.6 \pm 58.8	238.3 \pm 10.9
Correction (%)	29.3 \pm 17.7	46.3 \pm 39.8	33.3	30.9 \pm 12.5	33 \pm 7.2	9.6	3	27.8 \pm 23.1	0 \pm 0.1



Fig. 2 Type 1C: AP (left), lateral (middle) and 3-D CT (right) images depicting an example of a type 1C curve. This curve type features a coronal Cobb of $> 100^\circ$ and a sagittal Cobb $< 100^\circ$. The bisecting api-

cal horizontal line is depicted on the 3-D CT along with the UEV and LEV marked by star symbol

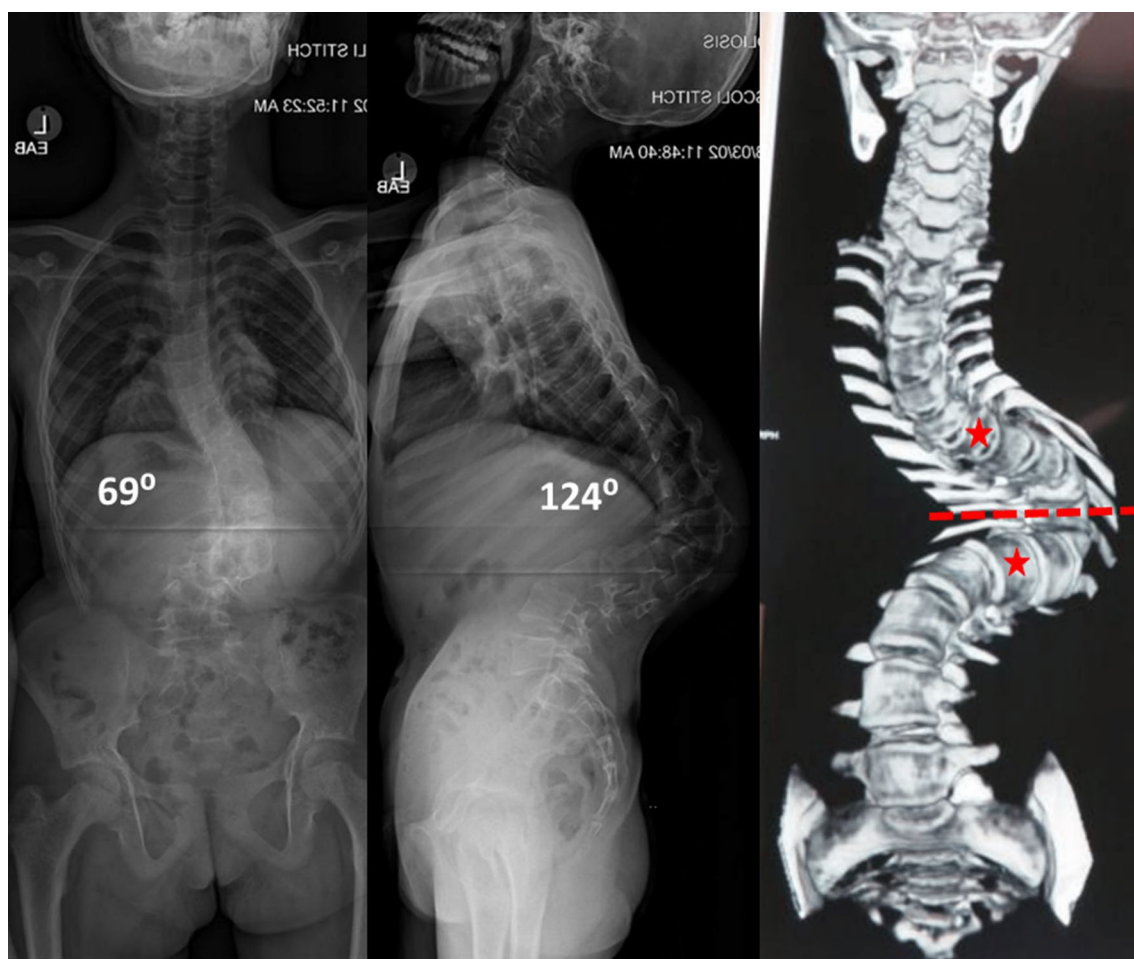


Fig. 3 Type 1S: AP (left), lateral (middle) and 3-D CT (right) images illustrating an example of a type 1S curve. This curve type has a coronal Cobb of $<100^\circ$ and sagittal Cobb $>100^\circ$. The bisecting apical

horizontal line is depicted on the 3-D CT along with the UEV and LEV marked by star symbol

Radiographic assessments and classification were performed by two fellowship trained spine surgeons.

As this study is a descriptive radiographic study, patient-reported outcomes are not provided in this study.

Classification principles

All patients with curve magnitude $>100^\circ$ were classified using a combination of erect AP/lateral X-rays and 3-D CT reconstruction. The 3-D CT reconstruction was a prerequisite for inclusion into this study due to the complex anatomic 3-D configuration of the deformities. The classification algorithm is shown in Fig. 1.

Type 1

The first step in the classification scheme was to identify on erect AP and lateral 36-inch radiographs if the major curve $>100^\circ$ exists in either the sagittal (1S) or coronal (1C)

plane or both (1CS). The second step required a CT reconstruction to identify the location of the proximal upper end vertebra (UEV) and distal lower end vertebra (LEV) of the major curve relative to the apical vertebra. A horizontal line is then drawn bisecting the apical vertebra. If the UEV and LEV remained above and below the horizontal line, respectively, the curve was assigned a prefix of 1 and was classified as either 1C (coronal curve $>100^\circ$, sagittal $<100^\circ$), 1S (sagittal $>100^\circ$, coronal $<100^\circ$) or 1CS (both coronal and sagittal $>100^\circ$).

Type 2

Any curvature in which the end vertebra was positioned at the level of, above or below the apical vertebra (horizontal line bisecting it), was assigned with a prefix number 2. If the UEV was positioned at the level of or below the bisecting horizontal apical line, the curve was classified as 2P. If the LEV was positioned at the level of or above

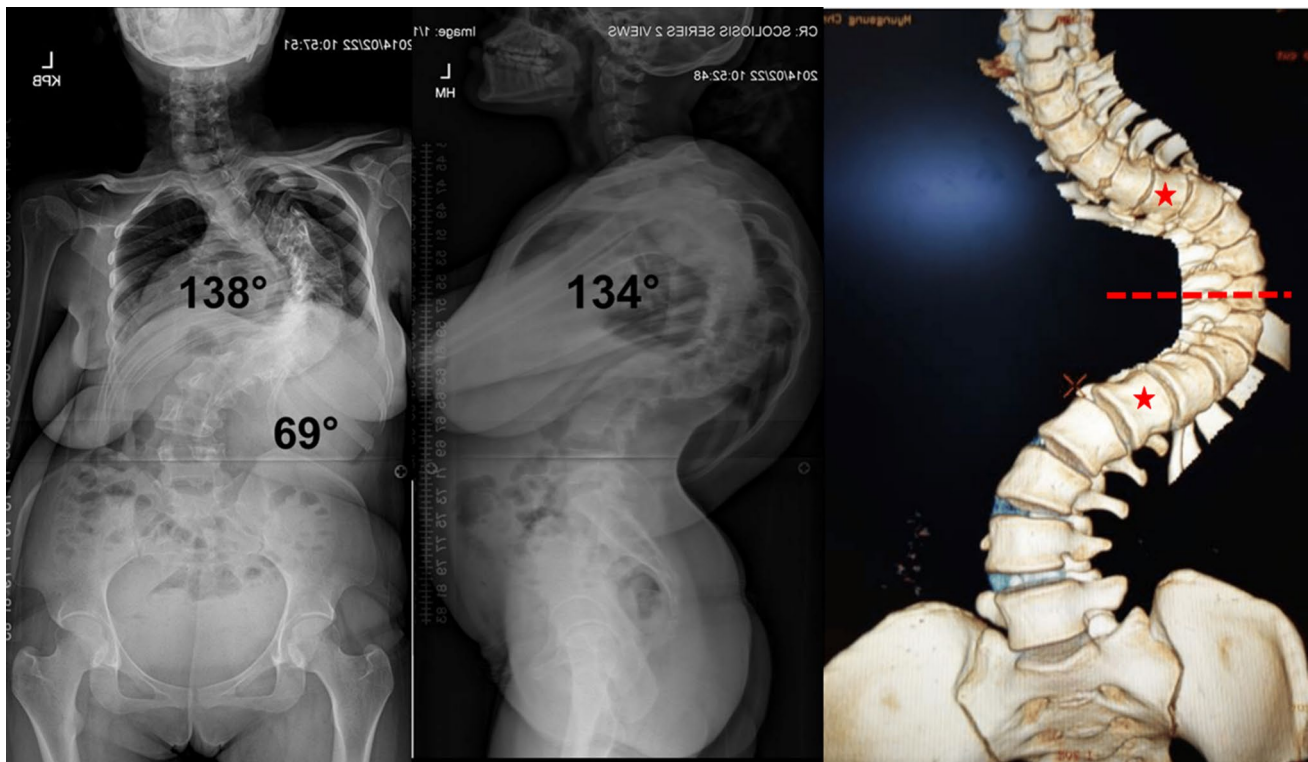


Fig. 4 Type 1CS: AP (left), lateral (middle) and 3-D CT (right) images illustrating an example of a type 1CS curve. This curve type has BOTH coronal and sagittal Cobb magnitudes of $>100^\circ$ and the

upper and lower end vertebrae positioned above and the bisecting apical horizontal line depicted on the 3-D CT along with the UEV and LEV marked by star symbol

the bisecting horizontal apical line, the curve was classified as 2D. If the UEV was positioned at the level of or below and the LEV was positioned at or above the bisecting horizontal apical line, the deformity was classified as 2PD. The resulting structure of this 2PD deformity assumes the shape of the Greek alphabet Omega (Ω) and as such we coined the term “omega deformity” to describe this subtype of severe kyphoscoliosis. Curves 2P and 2D curves do not form a full omega sign and as such referred to as “partial or pseudo-omega.”

Type 3

Type 3 curvatures were described as curves that exhibited vertebral transposition in the coronal and sagittal planes. The “transposition” implies complete displacement of a horizontal vertebral segment to lie side by side with the next segment. By virtue of demonstrating complete transposition, the sagittal Cobb measurement always exceeded $>180^\circ$. The shape of the resultant curve assumed the shape of the Greek alphabet “gamma (γ).” In the coronal plane, the transposition resembles a “bayonet.”

Type 4

Type 4 curves were the most severe type of curves. In the coronal plane, the spine consists of an upper vertical segment, a horizontal middle segment and a lower vertical segment, assuming the shape of the Greek letter “alpha (α).” In the sagittal plane, the curve resembles a gamma deformity, but the coronal plane exposes the hidden horizontal segment which is imperative to be recognized preoperatively.

Demographic, clinical and preoperative radiographic assessments

Demographic variables evaluated included age, gender, and body mass index (BMI). Preoperative diagnosis was classified as congenital, idiopathic, neuromuscular (NM), neurofibromatosis (NF). The length of preoperative halo-gravity traction was recorded.

Pre- and post-halo-gravity erect AP/lateral upright radiographic parameters were collected on all patients and included the major and minor coronal and sagittal Cobb angles, curve region (thoracic vs. thoracolumbar),

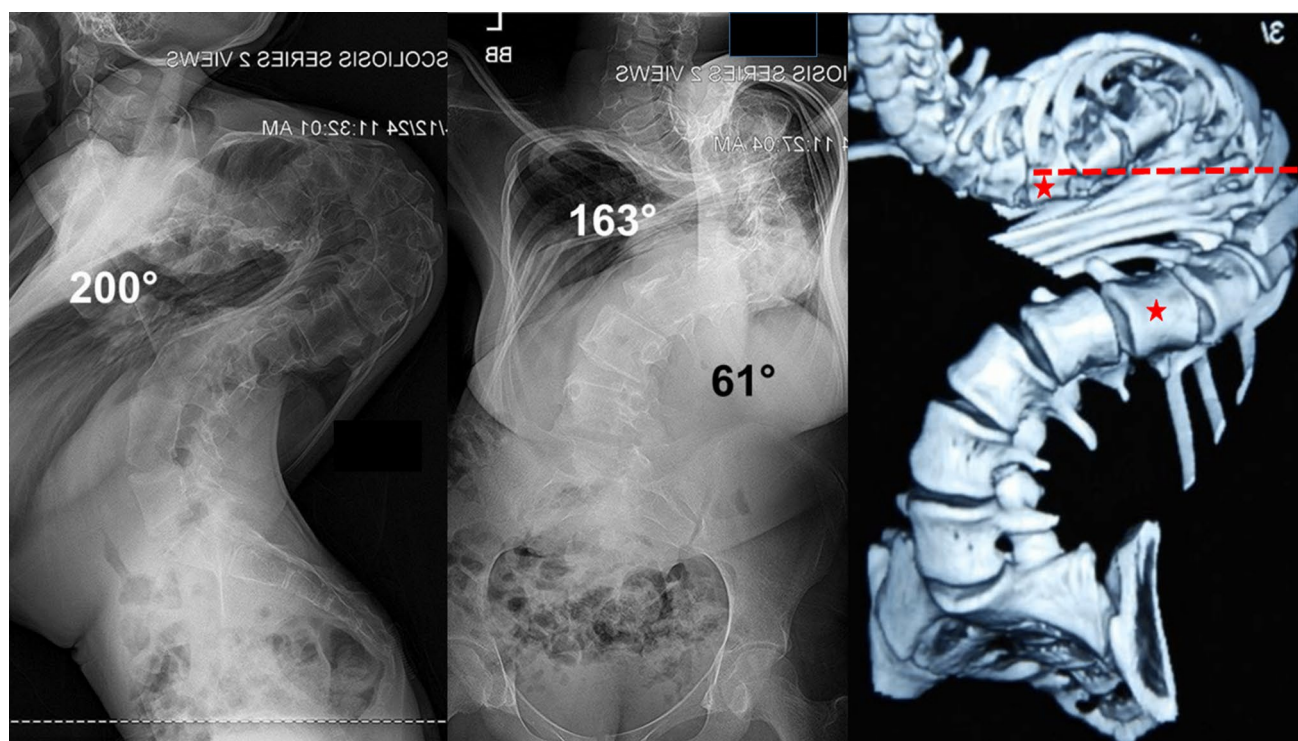


Fig. 5 Type 2P: lateral (left), AP (middle), 3-D CT (right) images depicting an example of a type 2P curve. This curve has both coronal and sagittal Cobb $> 100^\circ$. The proximal end vertebra is positioned at

the level of the bisecting apical horizontal line. The UEV and LEV are marked by star symbol

direction of curve (left or right), levels involved and Risser grade for skeletal maturity. 3-D CT scans with reconstruction were also performed for each patient and were instrumental in providing superior anatomical detail to accurately define each curvature.

Statistical analysis

Parametric data were expressed as mean \pm standard deviation (SD). Nonparametric data were expressed as median [interquartile range]. Statistical analysis was performed using JMP®, version 13. SAS Institute Inc., Cary, NC, 1989–2007.

Results

A total of 116 patients with curves $> 100^\circ$ were treated between 2012 and 2016. Ninety-eight (98) patients met the inclusion criteria and were classified into their respective categories using the aforementioned classification scheme detailed in the methods. The classification scheme yielded

a total of 4 main types (1, 2, 3 and 4) and 6 subtypes under types 1 and 2 (1C, 1S, 1CS, 2P, 2D and 2PD) (Table 1). A summary of demographic and radiographic data is shown in Tables 2 and 3, respectively. Post-halo-gravity radiographic results are shown in Table 4. A detailed analysis of each curve, its characteristics and response to halo-gravity traction is described below.

Subtype analysis

Type 1C

Type 1C in which the coronal curve alone measures $> 100^\circ$ is depicted in Fig. 2. Nine (8 females, 1 male, mean age 17.7 ± 3.7 years) out of 98 patients (9.1%) met this description. The most common diagnosis was idiopathic (6), followed by congenital (2) and neuromuscular (1). The mean coronal and sagittal Cobb angles were $120^\circ \pm 8.2^\circ$ and $81.6^\circ \pm 18.1^\circ$, respectively. All patients in this category underwent halo-gravity traction (mean 77.7 ± 59.5 days) and achieved a mean correction of $26 \pm 2.2\%$ in the coronal curve and $46.3 \pm 39.8\%$ in the sagittal curve.

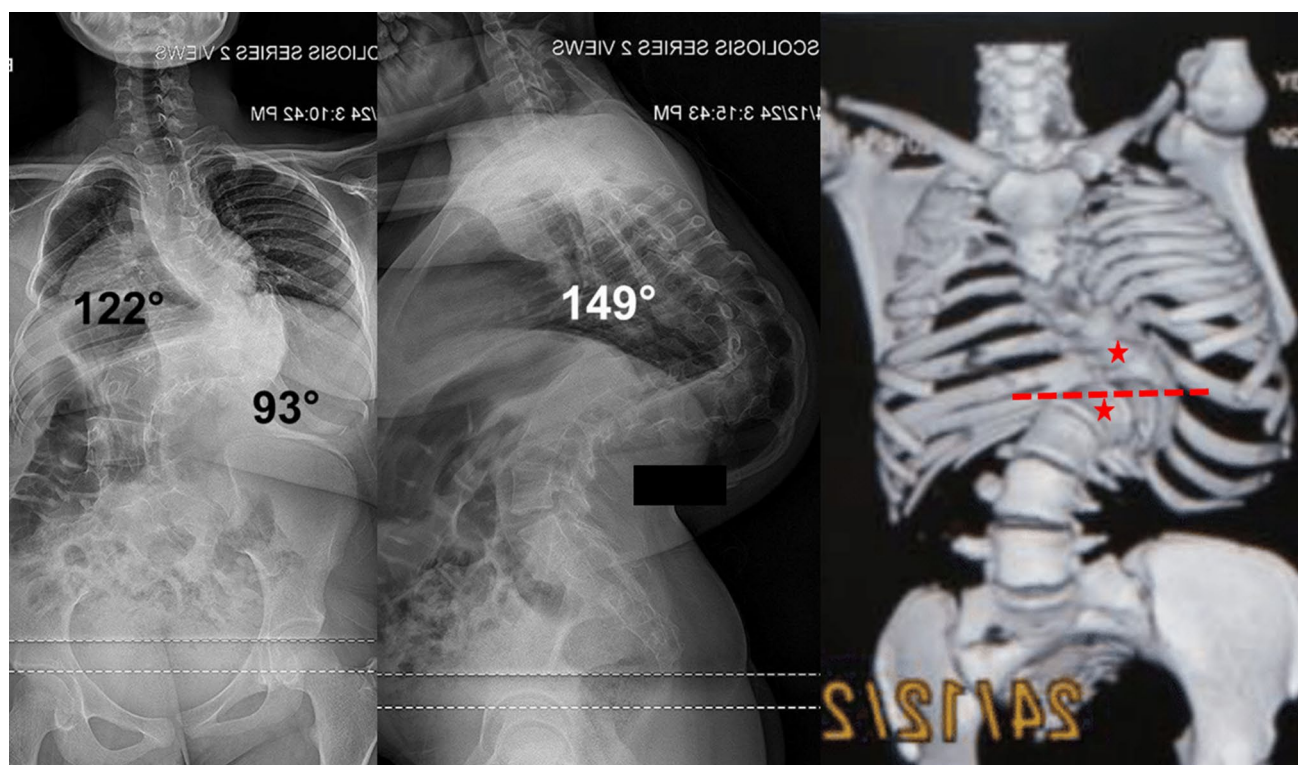


Fig. 6 Type 2D: AP (left), lateral (middle), 3-D CT (right) images depicting an example of a type 2D curve. This curve has both coronal and sagittal Cobb $> 100^\circ$. The distal end vertebra is positioned at the

level of the bisecting apical horizontal line. The UEV and LEV are marked by star symbol

Type 1S

Figure 3 shows an example of type 1S kyphoscoliosis described as having only the sagittal Cobb of $> 100^\circ$. There were 2 patients (2.6%), mean age 13.2 years, in this subtype, and both were diagnosed with congenital scoliosis. The mean coronal and sagittal Cobb angles were 79.6° and 113.2° , respectively. Both patients in this subtype underwent halo-gravity traction for 30 days which resulted in a mean correction of 30.5% and 33.3% in the coronal and sagittal curves, respectively.

Type 1CS

The 1CS (coronal $> 100^\circ$, sagittal $> 100^\circ$) is shown in Fig. 4. The 1CS represented the most common subtype in our cohort consisting of 43 patients (55%), 23 males and 20 females. The mean age was 17.5 ± 4 years. The diagnosis consisted of idiopathic (29), congenital (13) and neuromuscular (1). The mean coronal and sagittal Cobb angles were $127.7^\circ \pm 15.8^\circ$ and $131.8^\circ \pm 21.0^\circ$, respectively. All 43 patients in this category underwent halo-gravity traction (mean $82.4^\circ \pm 67.3^\circ$ days). The mean correction post-traction in the coronal and sagittal curves was $28.1 \pm 10.9\%$ and $30.9 \pm 12.5\%$, respectively.

Type 2P

Type 2P curves (coronal and/or sagittal curves $> 100^\circ$ with UEV positioned at or below the apical vertebra) are shown in Fig. 5. This group consisted of 21 patients (27%), 8 females, 13 males, mean age 18.9 ± 5.8 years. The diagnosis in this category consisted of 11 idiopathic, 6 congenital, 2 neuromuscular and 2 neurofibromatosis. The mean coronal and sagittal Cobb angles were $145.9^\circ \pm 27.6^\circ$ and $169.3^\circ \pm 14.5^\circ$, respectively. All patients underwent halo-gravity traction (mean 106 ± 42.9 days). The mean correction in the coronal and sagittal curves was $35.6 \pm 12.3\%$ and $33 \pm 7.2\%$.

Type 2D

Type 2D curves (coronal and/or sagittal curves $> 100^\circ$ with LEV positioned at or above the apical vertebra) consisted of 2 female patients (2.6%), mean age 19.5 years. The diagnosis in this category consisted of 1 idiopathic and 1 congenital scoliosis. The mean coronal and sagittal Cobb angles were 135.6° and 157.5° , respectively. Both patients in this subtype underwent halo-gravity traction for 72 days (mean) which resulted in a mean correction of 20.1% and 9.6% in the coronal and sagittal curves, respectively. A representative example of this subtype is shown in Fig. 6.

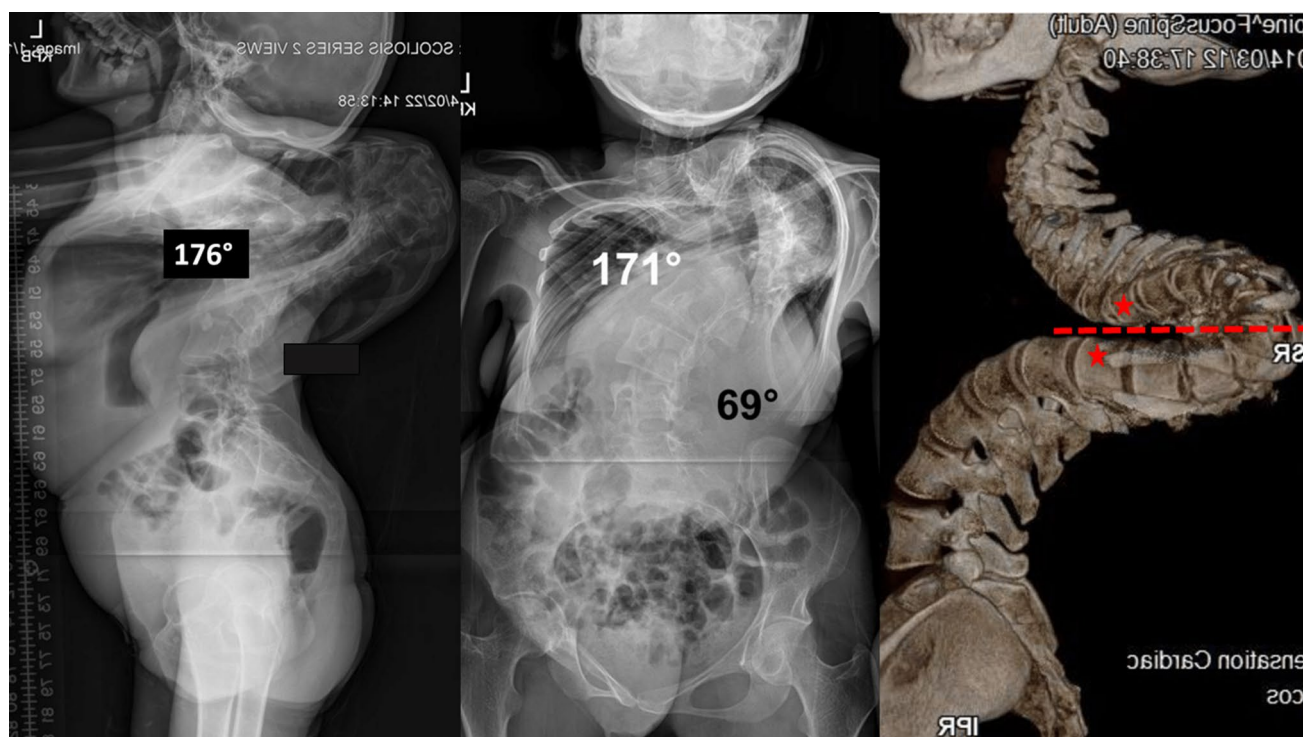


Fig. 7 Type 2PD (Omega Ω): lateral (left), AP (middle), 3-D CT (right) images depicting an example of a type 2PD curve. This curve has both coronal and sagittal Cobb $> 100^\circ$. Both the proximal and dis-

tal end vertebrae touch the bisecting apical horizontal line. The resulting structure of this deformity assumes the shape of the Greek alphabet Omega (Ω). The UEV and LEV are marked by star symbol

Type 2PD

The type 2PD curve (coronal and/or sagittal curves $> 100^\circ$ with both UEV and LEV are either positioned at the level of, below or above the apical vertebra) was the least common type of curve and consisted of only a 22-year-old female patient. The coronal and sagittal Cobb angles were 171° and 176° , respectively. After 205 days in traction, the curve improved by 22% and 3% in coronal and sagittal planes, respectively. Figure 7 illustrates the radiographs and 3-D reconstruction images for this patient.

Type 3: gamma (γ)

Type 3 curves exhibited a complete vertebral transposition in the sagittal plane (Fig. 8). There were 16 patients (9 female, 7 males), mean age of 17.9 ± 4.1 in this category. Unlike the omega deformities in which both coronal and sagittal curves are large in magnitude, the gamma (γ) curves principally occurs in the sagittal plane with little to no angular deformity in the coronal plane. The mean

sagittal Cobb was $216.7^\circ \pm 22.2^\circ$. The final measurement is reached by adding the angle subtended by the overlapping segments to 180° (Fig. 9). All patients underwent halo-gravity traction (mean 125 ± 49.6 days). The mean correction kyphosis following halo-traction was $157.8^\circ \pm 58.8^\circ$.

Type 4: alpha (α)

This curve type consisted of a vertical proximal segment, horizontal middle segment and a vertical distal segment represented the most severe of the curves (Fig. 10). Similar to gamma (γ) curves, this curve type can only be appreciated with a 3-D CT. A plain CT will underestimate the severity of this curve and could lead in inappropriate treatment. There were a total of 4 patients (2 males, 2 females), mean age 17.2 ± 4.2 . Using the gamma measurement technique, the mean preoperative sagittal Cobb was $238^\circ \pm 6.5^\circ$. The mean correction measurement following halo-traction was $238.3^\circ \pm 10.9^\circ$ indicating a lack of response to halo-traction in this subtype.



Fig. 8 Type 3 (gamma γ): AP (left), lateral (middle), 3-D CT coronal/sagittal (right) images depicting an example of a type 2PD curve. Type 3 curves exhibit a complete vertebral transposition in the sagittal plane and measured $>180^\circ$. The “transposition” implies com-

plete displacement of a horizontal vertebral segment to lie side by side with the next segment. The resulting structure of this deformity assumes the shape of the Greek alphabet gamma (γ)

Discussion

In this prospective case series of 78 patients with kyphoscoliosis exceeding 100° , we report a new radiographic classification to describe this complex deformity using erect AP/lateral X-rays and 3-D CT reconstructive radiographic images.

Classification schemes facilitate communication, research and aid in the development of treatment protocols for complex pathologies [1, 2]. The King–Moe and Lenke classifications are prime examples of the vitality of classification systems in expanding our understanding of the natural history and clinical characteristics of adolescent scoliosis [3, 4]. Severe kyphoscoliosis unlike AIS is infrequently encountered. The combination of its rare occurrence in many developed countries and paucity of the literature of its radiographic/clinical characteristics has contributed to the magnificent treatment challenges that it poses. As a prerequisite to gaining a thorough understanding of this complex deformity, we have attempted in this study to provide a descriptive radiographic analysis of these complex deformities. Whereas these severe forms of kyphoscoliosis were previously thought by many to be congenital in nature, we found that majority of patients (68%) in our cohort rather

harbored untreated early onset idiopathic scoliosis. This is a significant finding that provides some insight into the natural history of untreated early onset scoliosis.

Curve rigidity/flexibility is an integral part of the preoperative radiographic assessment of severe spinal deformity. Patients who are deemed to have rigid curves based on initial clinical exam and flexibility X-rays are recommended to undergo halo-gravity traction. In our cohort, all patients

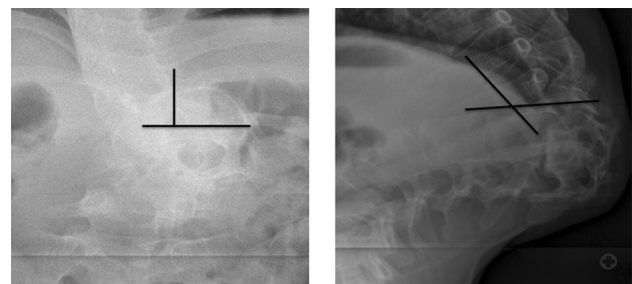


Fig. 9 Measurement technique for type 3 and type 4 curves: Due to complete vertebral transposition, standard Cobb measurement techniques cannot be used to measure type 3 and 4 curves. The final curve magnitude is reached by adding the angle subtended by the overlapping segments to 180°

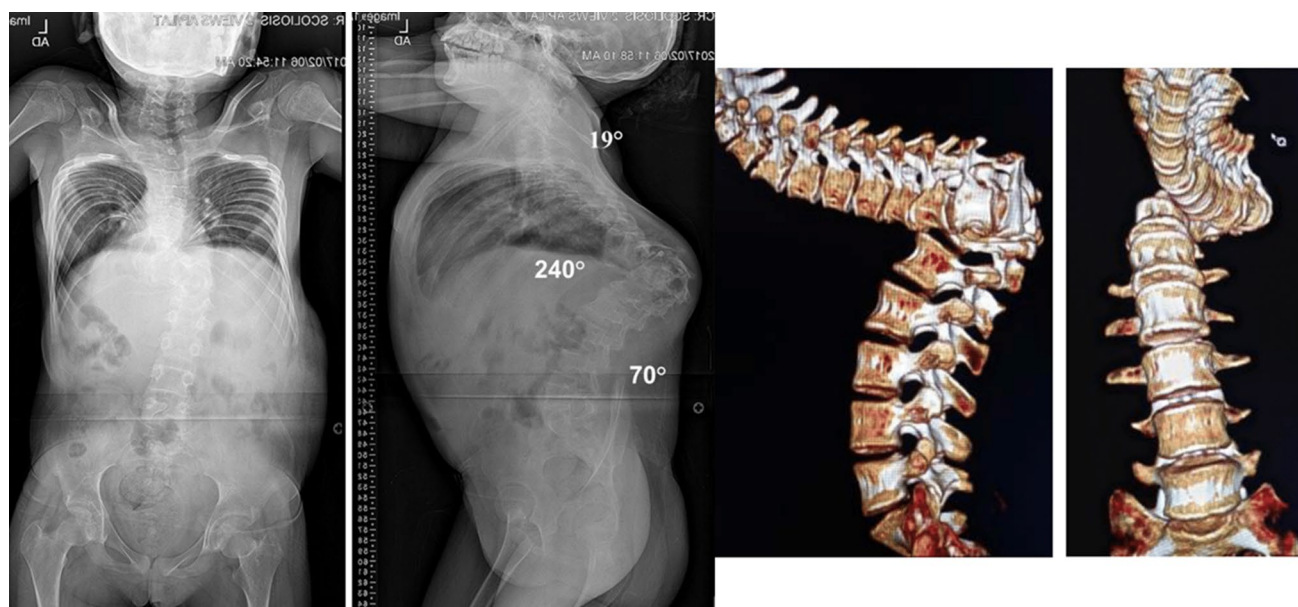


Fig. 10 Type 4 (alpha α): AP (left), lateral (middle), 3-D CT sagittal/coronal (right) images illustrating an example of a type 4 curve. In the coronal plane, the spine consists of an upper vertical segment,

a horizontal middle segment and a lower vertical segment, assuming the shape of the Greek alphabet (alpha α)

underwent halo-gravity traction (90 ± 60.4 days). The traction resulted in a mean improvement in the coronal and sagittal curve magnitude of 30 and 31.5%, respectively. Depending on the magnitude of improvement, patients with type 1 and 2 curves can change curve types into a less severe subtype. However, patients with type 3 and 4 curves maintain their primary curve morphology even with improvements following halo-traction. One can infer the impact that this improvement can make in the intraoperative positioning, achievement of optimal correction and perhaps reducing the need for complex three column osteotomies. Further, the impact of traction on improving pulmonary function has been previously reported [8–10].

The 3-D configuration of these severe deformities necessitates advanced imaging to be able to recapitulate the anatomic detail of each deformity. This is especially true for type 2, 3 and 4 curves. Plain radiographs inherently lack the anatomic detail necessary to understand the complex nature of these deformities. A unique feature of this classification scheme therefore is its reliance on 3-D CT reconstructions to provide superior bony anatomic detail. It is our firm belief that a solid understanding of the 3-D configuration of these deformities should be obtained prior to surgical intervention. With the advent of 3-D printing, a 3-D model can also be created to have a physical object with which one can plan a surgical procedure.

A strength of our proposed classification is the relative simplicity with only 4 main types. As we gain further in-depth understanding of each subtype and its clinical

implications, we anticipate modifications to occur. However, we hope this initial proposed classification will be useful as a systematic approach to evaluate and describe this unique subset of patients.

This study has limitations ensuing possible implications for its interpretation. First the number of patients included in this study is relatively small and therefore it is very plausible that other subtypes of complex kyphoscoliosis exist but not captured in this study. Second, due to the radiographic nature of this study, we did not report operative details and clinical outcomes. Further, there exists heterogeneity in the diagnosis of patients in this study and while, for example, two patients with different diagnosis may have the same radiographic classification, their underlying clinical diagnosis may completely change the clinical behavior of those curves. Lastly, it is worth mentioning that the definition of UEV and LEV was identified based on CT scans which were obtained in a recumbent position. In flexible curves, the true UEV and LEV may differ in the erect and recumbent positions and could potentially influence the choice of instrumented levels.

Conclusions

Severe kyphoscoliosis has been difficult to classify due to limitation of conventional radiographs. Our study describes a novel method of classifying the complex

kyphoscoliosis exceeding 100° using erect AP/lateral radiographs and 3-D CT reconstructive images. We hope that the descriptive analysis and classification will aid in expanding our understanding of these complex deformities.

Funding The paper was funded with a grant from K2M (Grant No: K2M/FC/060216).

Compliance with ethical standards

Conflict of interest Isaac O. Karikari is a consultant for Nuvasive and Depuy. Isaac O. Karikari receives fellowship funding from Nuvasive. For the remaining authors none were declared.

Open Access This article is distributed under the terms of the Creative Commons Attribution 4.0 International License (<http://creativecommons.org/licenses/by/4.0/>), which permits unrestricted use, distribution, and reproduction in any medium, provided you give appropriate credit to the original author(s) and the source, provide a link to the Creative Commons license, and indicate if changes were made.

References

1. Audigé L, Bhandari M, Hanson B, Kellam J (2005) A concept for the validation of fracture classifications. *J Orthop Trauma* 19:401–406
2. Garbuz DS, Masri BA, Esdaile J, Duncan CP (2002) Classification systems in orthopaedics. *J Am Acad Orthop Surg* 10:290–297
3. King HA, Moe JH, Bradford DS, Winter RB (1983) The selection of fusion levels in thoracic idiopathic scoliosis. *J Bone Joint Surg Am* 65:1302–1313
4. Lenke LG, Betz RR, Harms J, Bridwell KH, Clements DH, Lowe TG, Blanke K (2001) Adolescent idiopathic scoliosis: a new classification to determine extent of spinal arthrodesis. *J Bone Joint Surg Am* 83:1169–1181
5. Schwab F, Ungar B, Blondel B et al (2012) Scoliosis research society—Schwab adult spinal deformity classification: a validation study. *Spine* 37:1077–1082
6. Lamartina C, Berjano P (2014) Classification of sagittal imbalance based on spinal alignment and compensatory mechanisms. *Eur Spine J* 23:1177–1189
7. Berjano P, Lamartina C (2014) Classification of degenerative segment disease in adults with deformity of the lumbar or thoracolumbar spine. *Eur Spine J* 23:1815–1824
8. Koller H, Zenner J, Gajic V, Meier O, Ferraris L, Hitzl W (2012) The impact of halo-gravity traction on curve rigidity and pulmonary function in the treatment of severe and rigid scoliosis and kyphoscoliosis: a clinical study and narrative review of the literature. *Eur Spine J* 21:514–529
9. Li X, Zeng L, Li X, Chen X, Ke C (2017) Preoperative halo-gravity traction for severe thoracic kyphoscoliosis patients from Tibet: radiographic correction, pulmonary function improvement, nursing, and complications. *Med Sci Monit* 23:4021–4027
10. Rinella A, Lenke L, Whitaker C, Kim Y, Park SS, Peelle M, Edwards C 2nd, Bridwell K (2005) Perioperative halo-gravity traction in the treatment of severe scoliosis and kyphosis. *Spine* 30:475–482

Publisher's Note Springer Nature remains neutral with regard to jurisdictional claims in published maps and institutional affiliations.

Affiliations

Isaac Obiri Karikari¹ · Henry Pang² · Kwadwo Poku Yankey³ · Henry Ofori Duah³ · Harry Akoto³ · Rick Hodes⁴ · Oheneba Boachie-Adjei³ · FOCOS Spine Research Group³

✉ Isaac Obiri Karikari
Isaac.karikari@duke.edu

¹ Duke University Medical Center, DUMC Box 3807, Durham, NC 27710, USA

² Department of Orthopaedics and Traumatology, The University of Hong Kong, Sha Tin, Hong Kong

³ FOCOS Orthopedic Hospital, No 8 Teshie Street, Pantang, Accra, Ghana

⁴ American Jewish Joint Distribution Committee (JDC), Addis Ababa, Ethiopia